Neisch et al., https://doi.org/10.1083/jcb.201606082

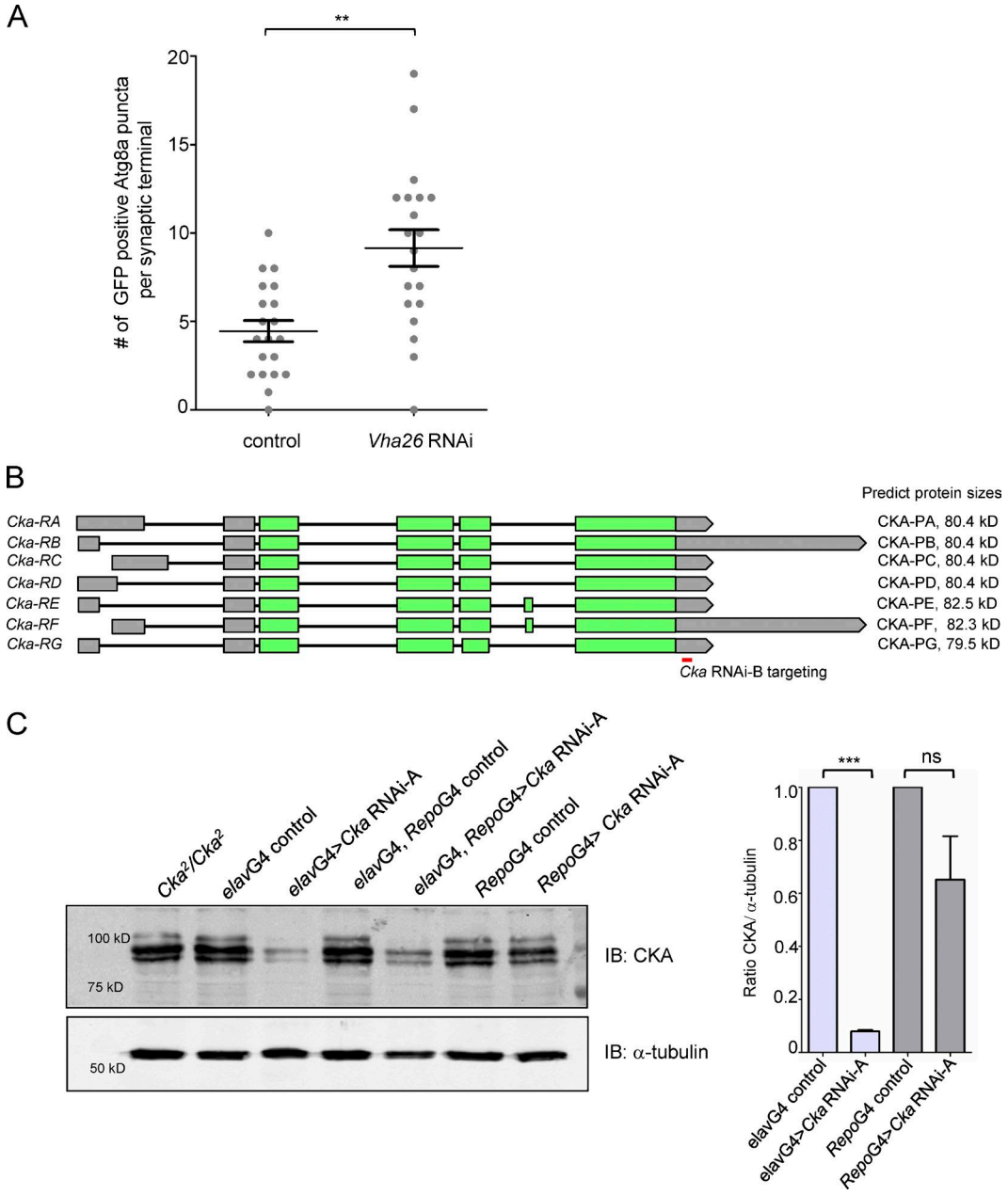

Figure S1. **Analysis of Atg8a puncta and characterization of *Cka* transcripts and proteins.** *mCh-GFP-Atg8a* was expressed in motoneurons using *Ok6-Gal4*. The number of GFP-positive Atg8a punctae in NMJ4 synaptic terminals was compared in control animals (*UAS-dicer2*) versus animals depleted of a V-ATPase subunit (*UAS-vha26* RNAi, *UAS-dicer2*). (A) Scatter plot of GFP-positive puncta numbers at the synaptic terminal. Each point in the graph represents the analysis of a single synaptic terminal. Bars indicate the mean and SEM for each genotype. Unpaired, two-tailed *t* test result: **, $P < 0.001$. (B) Transcripts of *Cka*. Green indicates the coding region. A red line indicates the shared region in the 3′ UTR targeted by the *Cka* RNAi-B line. Predicted protein isoform sizes are indicated to the right. (C) CKA protein in larval brain lysates is predominately present in neurons. Depletion of CKA in neurons by RNAi using the *elav-Gal4* driver resulted in diminished CKA protein levels compared with Cka^2 homozygous mutants and *elav-Gal4* control animals. RNAi depletion of CKA in glial cells by RNAi using the *Repo-Gal4* driver had no obvious effect on CKA protein levels compared with a *Repo-Gal4* control. Depletion of CKA in both neurons and glia had little effect on CKA protein levels compared with depletion in neurons alone. α-Tubulin was used as a loading control. In all RNAi cases (control and experimental), *UAS-dicer2* was coexpressed to increase RNAi efficiency. The graph shows the ratio of CKA to α-tubulin in CKA-depleted animals, normalized to controls set at 1.0. Data represent the mean and SEM of three separate experiments. IB, immunoblot. Paired, one-tailed *t* test results: ***, $P \leq 0.0001$; ns, not significant.

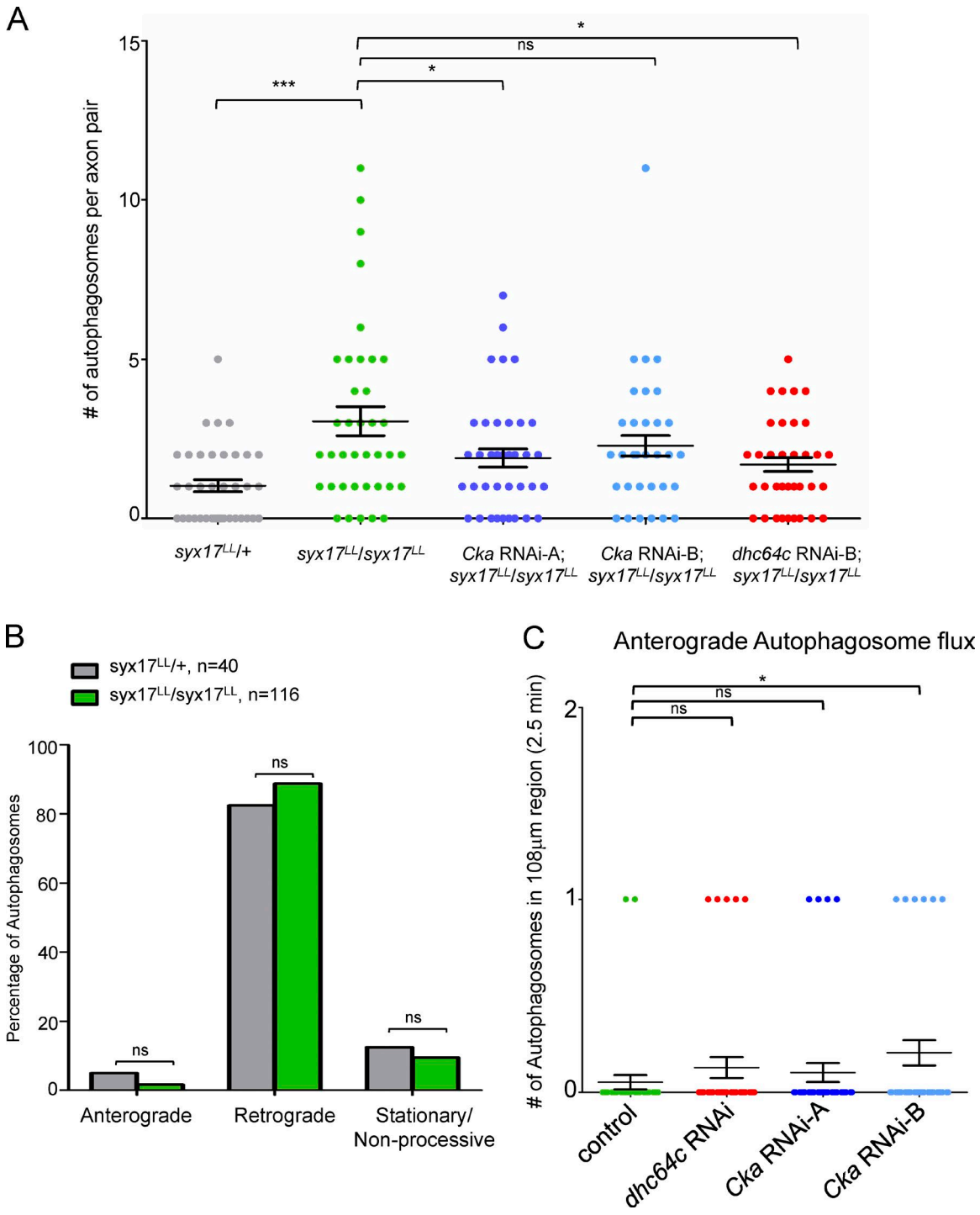

Figure S2. **Autophagosome number, anterograde flux, and motility in various genetic backgrounds.** (A) The number of autophagosomes per axon pair in the mid-axon region was increased in a syx17^{LL} homozygous mutant background. The number of autophagosomes per axon pair was decreased when either CKA or dynein was depleted by RNAi compared with *syx17^{LL}/syx17^{LL}* mutant controls. Each point represents the analysis from one kymograph of the number of autophagosomes captured in a 2.5-min video. The line for each genotype represents the mean, and error bars represent SEM. Unpaired, two-tailed *t* test results: *, P < 0.05; ***, P < 0.0001. (B) Genetically abolishing *syx17* did not affect the transport dynamics of autophagosomes compared with *syx17^{LL}/+* heterozygous controls. Berger's unconditional exact test results: ns, not significant. (C) Scatter plot of anterograde autophagosome flux measurements. Each point represents the analysis from one kymograph. Bars show the mean and SEM for each genotype. Unpaired, two-tailed *t* test result: *, P < 0.05. *n* = 39 axons for all except controls; *n* = 38 axons for controls.

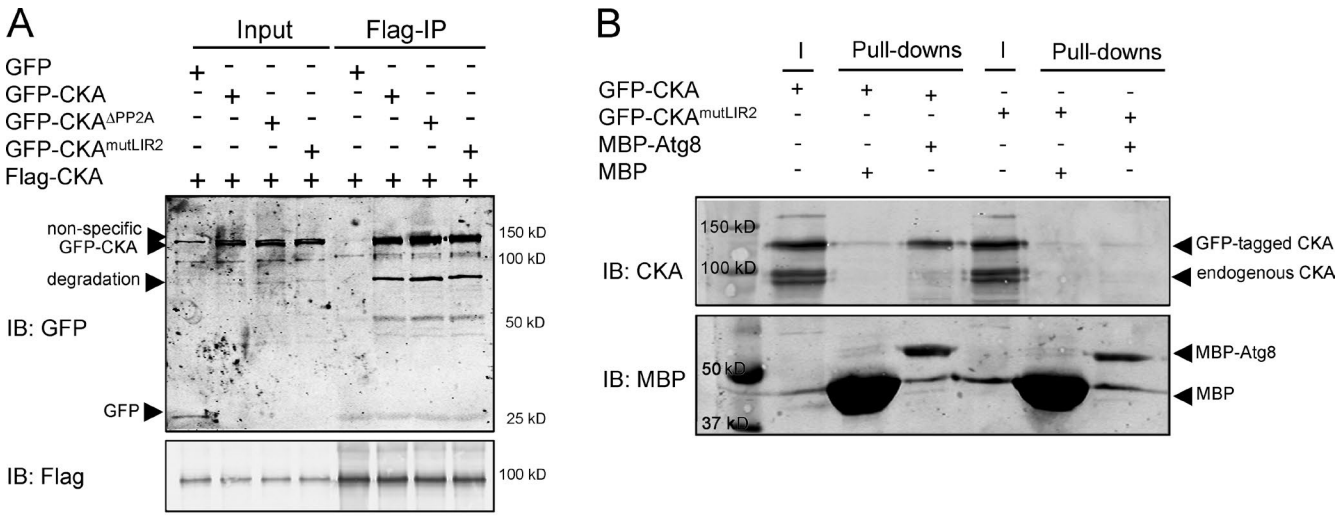

C

Genotype	Number of DCVs	Number net anterograde	Number net retrograde
control	50.75 +/- 2.50	23.08 +/- 1.53	23.25 +/- 1.72
dhc64c RNAi	15.92 +/- 1.61 ***	8.50 +/- 1.03 ***	3.92 +/- 1.18 ***
Cka RNAi-A	18.67 +/- 2.51 ***	8.00 +/- 1.17 ***	6.00 +/- 1.86 ***
Cka RNAi-B	30.75 +/- 3.00 ***	13.17 +/- 1.58 **	9.50 +/- 1.00 ***
Mob4 RNAi-A	26.17 +/- 2.10 ***	10.17 +/- 1.06 ***	9.92 +/- 1.66 ***
Strip RNAi-A	27.08 +/- 2.14 ***	13.67 +/- 1.51 **	8.33 +/- 1.59 ***

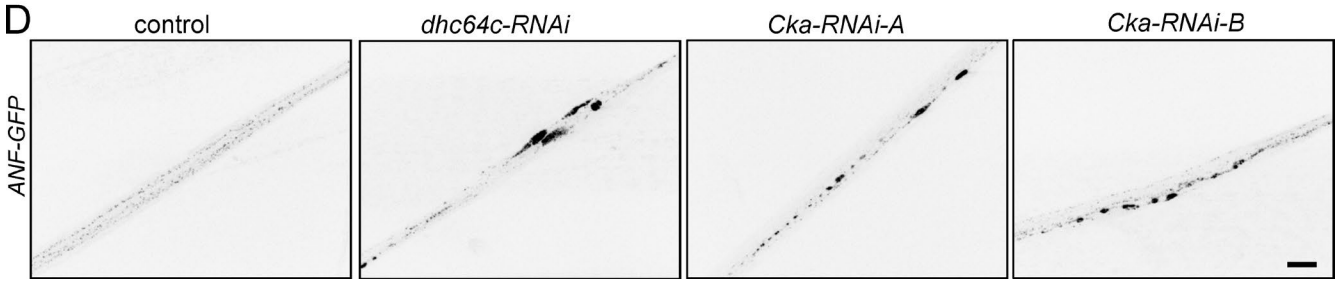

Figure S3. **CKA protein interactions and DCV motility.** (A) Flag-CKA was expressed in cultured *Drosophila* cells together with GFP-CKA, GFP-CKA$^{\Delta PP2A}$, GFP-CKA^{LIR2}, or GFP. GFP-CKA, GFP-CKA$^{\Delta PP2A}$, and GFP-CKA^{mutLIR2} coimmunoprecipitated with Flag-CKA–bound beads, whereas GFP did not. A representative blot is shown. $n = 3$ repeats. (B) GFP-CKA expressed in cultured *Drosophila* cells readily pulled down with MBP-Atg8a, but not with MBP. Mutating the LIR2 motif within CKA largely abolished the binding of GFP-CKA^{mutLIR2} to MBP-Atg8a compared with GFP-CKA. Endogenous CKA did not readily pull down with MBP-Atg8a. The low level of MBP-Atg8a protein may account for lack of pull-down of endogenous CKA. A representative blot is shown. $n = 2$ repeats. IB, immunoblot. (C) A chart of the mean number of DCVs and anterograde and retrograde DCV flux in controls and CKA-, Mob4-, Strip-, or dynein-depleted animals. DCVs were measured in an 80-µm region of the axon over 22.4 s. $n = 12$ axons. Unpaired, two-tailed *t* test results: **, $P < 0.005$; ***, $P \leq 0.0001$. (D) DCVs accumulate in axonal jams in the posterior regions of segmental nerves when CKA or dynein is depleted. Segmental nerves from control animals showed no accumulation of DCVs in axonal jams. DCVs were visualized by expressing *UAS-ANF-GFP* under the *Ok6-Gal4* motoneuron driver. Bar, 10 µm.

A

Genotype	Number of mitochondria	Number net anterograde	Number net retrograde
control	22.81 +/- 1.44	9.69 +/- 1.13	3.31 +/- 0.36
dhc64c RNAi	19.40 +/- 1.01	3.20 +/- 0.66 ***	0.33 +/- 0.13 ***
Cka RNAi-A	26.60 +/- 0.87 *	9.00 +/- 1.38	2.87 +/- 0.46
Cka RNAi-B	21.40 +/- 0.91	7.53 +/- 0.75	3.53 +/- 0.65
Mob4 RNAi-A	30.25 +/- 1.36 **	12.44 +/- 0.88	3.19 +/- 0.44
Strip RNAi-A	28.25 +/- 1.37 *	8.56 +/- 1.08	5.13 +/- 0.46 **

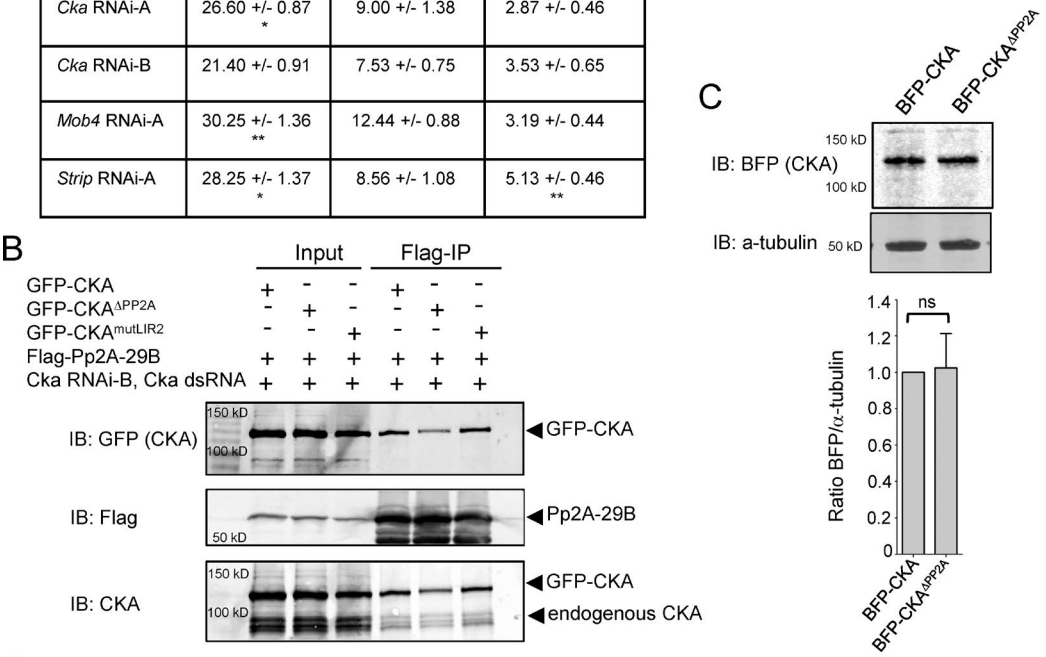

D

Genotype	Number of DCVs	Number net anterograde	Number net retrograde
control	50.75 +/- 2.496	23.08 +/- 1.525	23.25 +/- 1.723
Cka RNAi-B	30.75 +/- 2.998 ***	13.17 +/- 1.576 **	9.50 +/- 1.004 ***
Cka RNAi-B, *BFP-Cka*	43.75 +/- 4.612 ns *	16.50 +/- 1.545 * ns	16.92 +/- 2.414 * *
Cka RNAi-B, *BFP-Cka$^{\Delta PP2A}$*	25.42 +/- 1.905 *** ns	6.75 +/- 0.676 *** **	3.58 +/- 0.657 *** ***

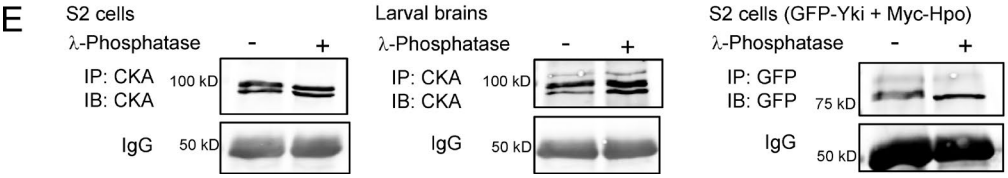

Figure S4. **Specificity and phosphoregulation of the STRIPAK complex.** (A) A chart of the mean number of mitochondria and anterograde and retrograde mitochondria flux in controls and in CKA-, Mob4-, Strip-, or dynein-depleted animals. Mitochondria were measured in an 80-µm region of the axon over 3 min and 21 s. Unpaired, two-tailed *t* test results: *, $P < 0.05$; **, $P < 0.005$; ***, $P \leq 0.0001$. $n = 15–16$ axons. (B) Flag–Pp2A-29B was expressed in cultured *Drosophila* cells together with GFP-CKA, GFP-CKA$^{\Delta PP2A}$, or GFP-CKA^{LIR2} while depleting endogenous CKA by RNAi (*Cka*RNAi-B and *Cka* double-strand RNA). GFP-CKA and GFP-CKA^{mutLIR2} coimmunoprecipitated with Flag–Pp2A-29B–bound beads. By comparision, GFP-CKA$^{\Delta PP2A}$ binding to Flag–Pp2A-29B–bound beads was reduced. Endogenous CKA was not completely depleted and also coimmunoprecipitates with Flag–Pp2A-29B. As CKA dimerizes, this is a likely explanation for the GFP-CKA$^{\Delta PP2A}$ binding seen. The blot was reprobed for endogenous CKA after probing for GFP-CKA. A representative blot is shown. $n = 3$ repeats. (C) BFP-CKA and BFP-CKA$^{\Delta PP2A}$ protein levels are similar when expressed in motoneurons depleted of endogenous CKA by expressing *UAS-CkaRNAi-B* using the *Ok6-Gal4* driver. The graph shows the ratio of BFP to α-tubulin. BFP-CKA levels were normalized to 1. Data represent the mean and SEM of three independent experiments. Paired, one-tailed *t* test results: ns, not significant. (D) A chart of the mean number of DCVs and anterograde and retrograde DCV flux in controls when CKA was depleted and when CKA was depleted while simultaneously coexpressing a BFP-CKA or BFP-CKA$^{\Delta PP2A}$ fusion protein. DCVs were measured in an 80-µm region of the axon over 22.4 s. Statistical significance of comparison for controls is shown in the top line and comparison to *Cka* RNA-B depletion in the second line. Unpaired, two-tailed *t* test results: *, $P < 0.05$; **, $P < 0.005$; ***, $P \leq 0.0001$; ns, not significant. $n = 12$ axons. (E) λ-Phosphatase treatment of immunoprecipitated CKA protein from cultured cells and larval brains does not collapse the multiple bands seen. GFP-Yki was immunoprecitated from cells expressing Myc-Hpo and GFP-Yki and treated with λ-phosphatase as a control. The IgG levels are shown as a loading control. Representative blots are shown. IB, immunoblot; IP, immunoprecipitate. $n = 2$ repeats.

Video 1. **Temporal *Cka* depletion in neurons.** Adult *Drosophila* on the left were uninduced (vehicle control), and the adults on the right were treated with 20 µg/ml RU-486 as early third instar larvae to induce *Cka* depletion in neurons. Video imaging was captured in real time with an iPhone5 (Apple Inc.) and compressed using HandBrake. The playback rate is 29.97 frames per second.

Video 2. **Temporal *Cka* depletion in neurons.** Adult *Drosophila* were treated with 20 µg/ml RU-486 as early third instar larvae to induce *Cka* depletion in neurons. Video imaging was captured in real time with an iPhone5 and compressed using HandBrake. The playback rate is 29.97 frames per second.

Video 3. **A sequence-specific RNAi off-target control for *Cka* temporally expressed in neurons.** Adult *Drosophila* on the left were uninduced (vehicle control), and the adults on the right were treated with 20 µg/ml RU-486 as early third instar larvae. Video imaging was captured in real time with an iPhone5 and compressed using HandBrake. The playback rate is 29.97 frames per second.

Video 4. **Temporal *Cka* depletion and rescue with a *BFP-Cka* fusion protein in neurons.** Adult *Drosophila* on the left were uninduced (vehicle control), and the adults on the right were treated with 20 µg/ml RU-486 as early third instar larvae to induce *Cka* depletion and expression of the *BFP-Cka* fusion protein in neurons. Video imaging was captured in real time with an iPhone5 and compressed using HandBrake. The playback rate is 29.97 frames per second.

Video 5. **Temporal *Cka* depletion and rescue with a *BFP-Cka*$^{\Delta PP2A}$ fusion protein in neurons.** Adult *Drosophila* on the left were uninduced (vehicle control), and the adults on the right were treated with 20 µg/ml RU-486 as early third instar larvae to induce *Cka* depletion and expression of the *BFP-Cka*$^{\Delta PP2A}$ fusion protein in neurons. Video imaging was captured in real time with an iPhone5 and compressed using HandBrake. The playback rate is 29.97 frames per second.

Video 6. **Temporal *Cka* depletion and rescue with a *BFP-Cka*$^{\Delta PP2A}$ fusion protein in neurons.** Adult *Drosophila* were treated with 20 µg/ml RU-486 as early third instar larvae to induce *Cka* depletion and expression of the *BFP-Cka*$^{\Delta PP2A}$ fusion protein in neurons. Video imaging was captured in real time with an iPhone5 and compressed using HandBrake. The playback rate is 29.97 frames per second.

Table S1. **Genotypes evaluated for each assay**

Genotypes evaluated for autophagic vesicle accumulation
D42-Gal4, UAS-mCh-Atg8, UAS-dicer2/+
UAS-CkaRNAi-A/+; D42-Gal4, UAS-mCh-Atg8, UAS-dicer2/+
UAS-CkaRNAi-B/+; D42-Gal4, UAS-mCh-Atg8, UAS-dicer2/+
UAS-CkaRNAi-C/+; D42-Gal4, UAS-mCh-Atg8, UAS-dicer2/+
D42-Gal4, UAS-mCh-Atg8, UAS-dicer2/UAS-CkaRNAi-D
UAS-CkaRNAi-B-C911/+; D42-Gal4, UAS-mCh-Atg8, UAS-dicer2/+
UAS-Mob4RNAi-A/+; D42-Gal4, UAS-mCh-Atg8, UAS-dicer2/+
D42-Gal4, UAS-mCh-Atg8, UAS-dicer2/UAS-Mob4RNAi-B
D42-Gal4, UAS-mCh-Atg8, UAS-dicer2/UAS-Mob4RNAi-C
UAS-StripRNAi-A/+; D42-Gal4, UAS-mCh-Atg8, UAS-dicer2/+
D42-Gal4, UAS-mCh-Atg8, UAS-dicer2/UAS-StripRNAi-B
D42-Gal4, UAS-mCh-Atg8, UAS-dicer2/UAS-StripRNAi-C
UAS-Ccm3RNAi-A/+; D42-Gal4, UAS-mCh-Atg8, UAS-dicer2/+
UAS-Ccm3RNAi-B/+; +/+; D42-Gal4, UAS-mCh-Atg8, UAS-dicer2/+
UAS-Ccm3RNAi-C/+; D42-Gal4, UAS-mCh-Atg8, UAS-dicer2/+
D42-Gal4, UAS-mCh-Atg8, UAS-dicer2/UAS-hpoRNAi-A
UAS-hpoRNAi-B/+; D42-Gal4, UAS-mCh-Atg8, UAS-dicer2/+
UAS-CkaRNAi-A/+; D42-Gal4, UAS-mCh-Atg8, UAS-dicer2/UAS-hpoRNAi-A
D42-Gal4, UAS-mCh-Atg8, UAS-dicer2/UAS-Flag-hpo
D42-Gal4, UAS-mCh-Atg8, UAS-dicer2/UAS-Flag-hpo^{T195E}
D42-Gal4, UAS-mCh-Atg8, UAS-dicer2/UAS-BFP-Cka
D42-Gal4, UAS-mCh-Atg8, UAS-dicer2/UAS-BFP-Cka$^{\Delta PP2A}$
Cka^{2}/Cka^{2}; D42-Gal4, UAS-mCh-Atg8/+
D42-Gal4, UAS-mCh-Atg8, UAS-dicer2/UAS-mts^{DN}
D42-Gal4, UAS-mCh-Atg8, UAS-dicer2/UAS-Pp2A-29BRNAi
UAS-mCh-GFP-Atg8/+; elavSwitch/+
UAS-mCh-GFP-Atg8/+; elavSwitch/UAS-Pp2A-29BRNAi
UAS-mCh-GFP-Atg8/+; elavSwitch/UAS-mtsRNAi
UAS-mCh-GFP-Atg8/+; elavSwitch/UAS-mts^{DN}
Genotypes evaluated for autophagosome transport
M12Gal4, UAS-mCh-GFP-Atg8, syx17^{LL}/syx17^{LL}
M12Gal4, UAS-mCh-GFP-Atg8, syx17^{LL}/+
UAS-CkaRNAi-B/+; M12Gal4, UAS-mCh-GFP-Atg8, syx17^{LL}/syx17^{LL}
UAS-CkaRNAi-A/+; M12Gal4, UAS-mCh-GFP-Atg8, syx17^{LL}/syx17^{LL}
M12Gal4, UAS-mCh-GFP-Atg8, syx17^{LL}/syx17^{LL}, UAS-dhc64cRNAi
Genotypes evaluated for mitochondrial transport
M12-Gal4, UAS-GFP-HA-mito/UAS-dicer2
M12-Gal4, UAS-GFP-HA-mito/UAS-dhc64cRNAi
UAS-CkaRNAi-A/+; M12-Gal4, UAS-GFP-HA-mito/UAS-dicer2
UAS-CkaRNAi-B/+; M12-Gal4, UAS-GFP-HA-mito/+
UAS-Mob4RNAi-A/+; M12-Gal4, UAS-GFP-HA-mito/UAS-dicer2
UAS-StripRNAi-A/+; M12-Gal4, UAS-GFP-HA-mito/UAS-dicer2
Genotypes evaluated for DCV transport
SG26.1-Gal4, UAS-ANF-GFP/+
SG26.1-Gal4, UAS-ANF-GFP/UAS-dhc64cRNAi
UAS-CkaRNAi-A/+; SG26.1-Gal4, UAS-ANF-GFP/UAS-dicer2
UAS-CkaRNAi-B/+; SG26.1-Gal4, UAS-ANF-GFP/+
UAS-Mob4RNAi-A/+; SG26.1-Gal4, UAS-ANF-GFP/UAS-dicer2
UAS-StripRNAi-A/+; SG26.1-Gal4, UAS-ANF-GFP/UAS-dicer2
UAS-CkaRNAi-B/+; SG26.1-Gal4, UAS-ANF-GFP/UAS-BFP-Cka
UAS-CkaRNAi-B/+; SG26.1-Gal4, UAS-ANF-GFP/UAS-BFP-Cka$^{\Delta PP2A}$
Genotypes evaluated for Atg8a puncta distribution
Ok6-Gal4, UAS-mCh-GFP-Atg8/+; UAS-dicer2/+
Ok6-Gal4, UAS-mCh-GFP-Atg8/UAS-vha26RNAi; UAS-dicer2/+

Table S1. **Genotypes evaluated for each assay** *(Continued)*

Genotypes evaluated for autophagosome accumulation volumetric analysis
Ok6-Gal4, UAS-mCh-GFP-Atg8/+
Ok6-Gal4, UAS-mCh-GFP-Atg8/+; UAS-dhc64cRNAi/+
Ok6-Gal4, UAS-mCh-GFP-Atg8/+; UAS-dhc64cRNAi/UAS-Atg1^{K38Q}
Genotypes evaluated after temporal neuronal depletion
UAS-CkaRNAi-B-C911/+; elav-Switch/+
UAS-CkaRNAi-B/+; elav-Switch/+
UAS-CkaRNAi-B/+; elav-Switch/UAS-BFP-Cka
UAS-CkaRNAi-B/+; elav-Switch/UAS-BFP-Cka$^{\Delta PP2A}$